Inorg. Chem. **2006**, *45*, 6875–6883

Inorganic Chemistry

Article

Structural, Redox, and Photophysical Studies of the Tetra(pyridyl)porphyrin Complex Containing Four (2,2′-Bipyridine)(2,2′:6′,2′′-terpyridine)ruthenium(II) Groups

Hiroki Kon, Kiyoshi Tsuge,* Taira Imamura, Yoichi Sasaki,* Shoji Ishizaka, and Noboru Kitamura*

Division of Chemistry, Graduate School of Science, Hokkaido University,
Sapporo 060-0810, Japan

Received February 19, 2006

New hybrid complexes of polypyridyl ruthenium and pyridylporphyrins have been prepared by the coordination of pyridyl nitrogens to the ruthenium centers. A 1:4 hybrid complex, $[\{Ru(bpy)(trpy)\}_4(\mu_4\text{-}H_2Py_4P)]^{8+}$ ($[\mathbf{1}]^{8+}$) (bpy = 2,2′-bipyridine; trpy = 2,2′:6′,2′′-terpyridine; H_2Py_4P = 5,10,15,20-tetra(4-pyridyl)porphyrin), has been characterized by the single-crystal X-ray diffraction method. A 1:1 complex, $[\{Ru(bpy)(trpy)\}(H_2PyT_3P)]^{2+}$ ($[\mathbf{2}]^{2+}$) (H_2PyT_3P = 5-(4-pyridyl)tritolylporphyrin) has also been prepared. The Soret band of the porphyrin ring shifts to longer wavelength with some broadening, the extent of the shift being larger for $[\mathbf{1}]^{8+}$. Cyclic voltammograms of the two complexes show simple overlap of the component redox waves. The complexes are weakly emissive at room temperature, which becomes stronger at lower temperatures. While $[\mathbf{1}]^{8+}$ at >140 K and $[\mathbf{2}]^{2+}$ at 77–280 K show only porphyrin fluorescence, $[\mathbf{1}]^{8+}$ at <140 K shows ruthenium and porphyrin phosphorescence, in addition to the porphyrin fluorescence.

Introduction

Pyridylporphyrins are intriguing ligands that yield, when coordinated to metal porphyrin complexes or to other metal complexes, unique supramolecular assemblies with multielectron redox and photochemical activities.[1−3] The hybrid complexes with polypyridylruthenium(II) centers are particularly interesting because they have two types of emissive chromophores in direct connection and provide us with important information on the excited-state energetics between them.[4] The complexes of 5,10,15,20-tetra(pyridyl)porphyrin (H_2Py_4P) and their analogues with four polypyridylruthenium(II) moieties have been extensively studied by Araki, Toma, and their co-workers.[5] Essential features of their studies may be summarized as follows. (i) The energy levels of the two chromophores are very close and the order is easily reversed by the introduction of appropriate substituents or the axial ligands on metal centers in the porphyrin ring. (ii) Porphyrin fluorescence is usually observed, while the emission from the ruthenium(II) centers are largely quenched

---

* To whom correspondence should be addressed. E-mail: tsuge@sci.hokudai.ac.jp (K.T.); ysasaki@sci.hokudai.ac.jp (Y.S.); kitamura@sci.hokudai.ac.jp (N.K.).

(1) Imamura, T.; Fukushima, K. *Coord. Chem. Rev.* **2000**, *198*, 133−156.

(2) (a) Kimura, A.; Funatsu, K.; Kido, H.; Imamura, T.; Sasaki, Y. *Chem. Lett*. **1995**, *24*, 207−208. (b) Funatsu, K.; Kimura, A.; Imamura, T.; Sasaki, Y. *Chem. Lett*. **1995**, *24*, 765−766. (c) Kariya, N.; Imamura, T.; Sasaki, Y. *Inorg. Chem*. **1997**, *36*, 833−839. (d) Funatsu, K.; Kimura, A.; Imamura, T.; Ichimura, A.; Sasaki, Y. *Inorg. Chem*. **1997**, *36*, 1625−1635. (e) Kariya, N.; Imamura, T.; Sasaki, Y. *Inorg. Chem*. **1998**, *37*, 1658−1660. (f) Funatsu, K.; Imamura, T.; Ichimura, A.; Sasaki, Y. *Inorg. Chem*. **1998**, *37*, 1798−1804. (g) Funatsu, K.; Imamura, T.; Ichimura, A.; Sasaki, Y. *Inorg. Chem*. **1998**, *37*, 4986−4995. (h) Okumura, A.; Funatsu, K.; Sasaki, Y.; Imamura, T. *Chem.* Lett. **1999**, 28, 779−780. (i) Imamura, T.; Funatsu, K.; Ye, S.; Morioka, Y.; Uosaki, K.; Sasaki, Y. *J. Am. Chem. Soc.* **2000**, *122*, 9032−9033. (j) Itasaka, A.; Abe, M.; Yoshimura, T.; Tsuge, K.; Suzuki, M.; Imamura, T.; Sasaki, Y. *Angew. Chem., Int. Ed.* **2002**, *41*, 463−466. (k) Fukushima, K.; Funatsu, K.; Ichimura, A.; Sasaki, Y.; Suzuki, M.; Fujihara, T.; Tsuge, K.; Imamura, T. *Inorg. Chem.* **2003**, *42*, 3187−3193. (l) Suzuki, M.; Tsuge, K.; Sasaki, Y.; Imamura, T. *Chem. Lett.* **2003**, *32*, 564−565.

(3) For some related porphyrin−ruthenium(polypyridine) hybrids, see: (a) Lintuluoto, J. M.; Borovkov, V. V.; Inoue, Y. *Tetrahedron Lett.* **2000**, *41*, 4781−4786. (b) Hu, Y.-Z.; Tsukiji, S.; Shinkai, S.; Oishi, S.; Hamachi, I. *J. Am. Chem. Soc.* **2000**, *122*, 241−253.

(4) (a) Odobel, F.; Zabri, H. *Inorg. Chem.* **2005**, *44*, 5600−5611. (b) Wilson, G. J.; Launikonis, A.; Sasse, W. H. F.; Mau, A. W.-H. *J. Phys. Chem. A* **1997**, *101*, 4860−4866. (c) de Carvalho, I. M. M.; Moreira, Í. de S.; Gehlen, M. H. *Inorg. Chem.* **2003**, *42*, 1525−1531. (d) Kozlov, D. V.; Tyson, D. S.; Goze, C.; Ziessel, R.; Castellano, F. N. *Inorg. Chem.* **2004**, *43*, 6083−6092.

(5) (a) Araki, K.; Toma, H. E. *J. Photochem. Photobiol. A* **1994**, *83*, 245−250. (b) Araki, K.; Wagner, M. J.; Wrighton, M. S. *Langumuir* **1996**, *12*, 5393−5398. (c) Toma, H. E.; Araki, K. *Coord. Chem. Rev.* **2000**, *196*, 307−329. (d) Araki, K.; Losco, P.; Engelmann, F. M.; Winnischofer, H.; Toma, H. E. *J. Photochem. Photobiol. A* **2001**, *142*, 25−30.

10.1021/ic0602852 CCC: $33.50

Scheme 1. Schematic View of the Porphyrin−Ruthenium Hybrid Complexes Prepared in This Study

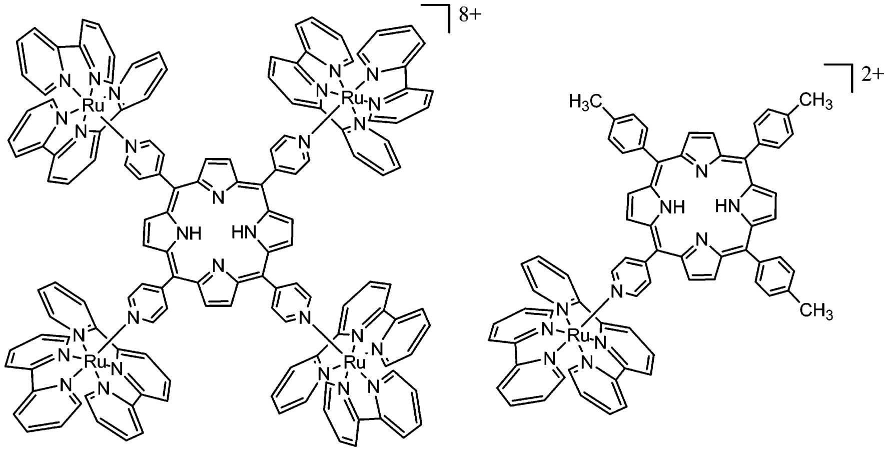

$[\mathbf{1}]^{8+}$ $[\mathbf{2}]^{2+}$

by the electron transfer to the porphyrin group. (iii) In one case, porphyrin phosphorescence was observed at 77 K which is associated with ruthenium(II) absorption rather than the porphyrin $\pi-\pi^*$ transitions. These results show some significant and promising aspects of these hybrid complexes, but clearly further studies from a more photophysical point of view are required to understand the overall profiles of the photoexcited-state decay.

In this paper, we wish to report a new member of the tetra(pyridyl)porphyrin complex containing four (bpy)(trpy) ruthenium(II) units, $[\{\mathrm{Ru(bpy)(trpy)}\}_4(\mu_4\text{-}\mathrm{H_2Py_4P})]^{8+}$ ($[\mathbf{1}]^{8+}$) (bpy = 2,2′-bipyridine; trpy = 2,2′:6′,2″-terpyridine) (Scheme 1). The 1:1 hybrid complex $[\mathrm{Ru(bpy)(trpy)(H_2PyT_3P)}]^{2+}$ ($[\mathbf{2}]^{2+}$) was also prepared for comparison. We have carried out the phtophysical measurements of these complexes and revealed details of excited-state decay processes by observing all the possible emission types of these hybrid complexes. The X-ray crystal structure of $[\mathbf{1}]^{8+}$ has been made for the first time for this type of 1:4 aggregate.

Experimental Section

Materials. Reagents, including $\mathrm{H_2Py_4P}$, were purchased from WAKO, ACROS, Dojin, and Aldrich. All reagents were used without further purification unless noted. The ruthenium complex $[\mathrm{Ru(bpy)(trpy)(H_2O)}](\mathrm{PF_6})_2$[6] and $\mathrm{H_2PyT_3P}$[7] were prepared according to literature procedures. Tetra-*n*-butylammonium hexafluorophosphate, $[n\text{-}\mathrm{Bu_4N}]\mathrm{PF_6}$, was recrystallized twice from ethanol. Solvents for the electrochemical measurements were distilled from calcium hydride under argon. For the photophysical measurements, spectrograde solvents (Dojin) were used.

Preparations of the Complexes. 5,10,15,20-Tetrakis{(2,2′-bipyridine)-(2,2′:6′,2″-terpyridine)ruthenium}(4-pyridyl)-porphyrin, $[\{\mathbf{Ru(bpy)(trpy)}\}_4(\mu_4\text{-}\mathbf{H_2Py_4P})](\mathbf{PF_6})_8\cdot 2\mathbf{CHCl_3}\cdot \mathbf{CH_3COCH_3}$. The aqua complex, $[\mathrm{Ru(bpy)(trpy)(H_2O)}](\mathrm{PF_6})_2$ (75.9 mg, 0.095 mmol), and the ligand $\mathrm{H_2Py_4P}$ (14.7 mg, 0.024 mmol) were dissolved in a mixed solvent of acetone−chloroform (1:1 v/v, 80 $\mathrm{cm^3}$), and the solution was refluxed for 43 h. The solid deposited on the wall of the reaction vessel during the reflux was occasionally redissolved in the solution. After the filtration at room temperature, the filtrate was evaporated to a half volume. After the solution was left to stand overnight, fine needles deposited, which were collected by filtration. Yield: 16.3 mg (18%). Found: C, 43.00; H, 2.92; N, 9.84%. Calcd for $[\{\mathrm{Ru(bpy)(trpy)}\}_4(\mathrm{H_2Py_4P})](\mathrm{PF_6})_8\cdot 2\mathrm{CHCl_3}\cdot \mathrm{CH_3COCH_3}$: C, 43.14; H, 2.75; N, 9.71%. The product was soluble in acetone, slightly soluble in dichloromethane and water, and sparingly soluble in $\mathrm{CHCl_3}$. ^{1}H NMR (acetone-d_6): δ 9.50 (d, 4H, bpy), 9.08 (d, 4H, bpy), 9.00 (d, 8H, trpy), 8.80−8.88 (m, 12H, trpy, bpy), 8.67 (br, 8H, β), 8.4−8.59 (m, 16H, trpy, bpy, py), 8.20−8.33 (m, 20H, trpy, bpy), 8.02−8.12 (m, 12H, bpy, py), 7.78 (d, 4H, bpy), 7.67 (t, 8H, trpy), 7.35 (t, 4H, bpy), −3.35 (s, 2H, por-NH).

5-[{(2,2′-Bipyridine)(2,2′:6′,2″-terpyridine)ruthenium}(4-pyridyl)-tritolylporphyrin, $[\{\mathbf{Ru(bpy)(trpy)}\}(\mathbf{H_2PyT_3P})](\mathbf{PF_6})_2$ ($[\mathbf{2}](\mathbf{PF_6})_2$). The aqua complex, $[\mathrm{Ru(bpy)(trpy)(H_2O)}](\mathrm{PF_6})_2$ (59.6 mg, 0.075 mmol), was dissolved in 15 $\mathrm{cm^3}$ of acetone. A $\mathrm{CH_2Cl_2}$ solution (15 $\mathrm{cm^3}$) of $\mathrm{H_2PyT_3P}$ (49.0 mg, 0.075 mmol) was added to the solution. The mixture was refluxed for 72 h, and then it was evaporated to ca. 10 $\mathrm{cm^3}$. To the concentrate was added 12.2 mg (0.075 mmol) of $\mathrm{NH_4PF_6}$ dissolved in a small amount of acetone, and then the mixture was left over the moisture of diethyl ether. The solid material deposited was collected by filtration after 1 d. Yield: 94.3 mg (87%). Found: C, 59.04; H, 3.84; N, 9.65%. Calcd for $[\{\mathrm{Ru(bpy)(trpy)}\}(\mathrm{H_2PyT_3P})](\mathrm{PF_6})_2$: C, 59.29; H, 3.78; N, 9.74%. FAB MS: $m/z = 1439$. ^{1}H NMR (acetone-d_6): δ 9.56 (d, 1H, bpy), 9.09 (d, 1H, bpy), 9.05 (d, 2H, trpy), 8.80−8.92 (m, 10H, trpy, bpy, β), 8.68 (br, 2H, β), 8.50−8.60 (m, 3H, bpy, py), 8.36 (d, 2H, py), 8.22−8.31 (m, 5H, trpy, bpy), 8.03−8.12 (m, 7H, bpy, py, tol), 7.78 (d, 1H, bpy), 7.70 (t, 2H, trpy), 7.65 (d, 6H, tol), 7.34 (t, 1H, bpy), 2.71 (s, 9H, tol), −2.88 (s, 2H, por-NH).

Measurements. UV−vis absorption spectra were recorded on Hitachi U3410 and U3000 spectrophotometers. ^{1}H NMR spectra were measured at room temperature with a JEOL JNM-EX270 spectrometer. Cyclic voltammograms were measured with a HOKUTO HZ-300 cyclic voltammetric analyzer at a scan rate of 100 mV/s. The working and counter electrodes were a platinum disk ($[\mathbf{1}]^{8+}$) or glassy-carbon disk ($[\mathbf{2}]^{2+}$) and a platinum wire, respectively. For the measurements on $[\mathbf{1}]^{8+}$, the sample solutions (ca. 0.001 M) in 0.1 M $[n\text{-}\mathrm{Bu_4N}]\mathrm{PF_6}$−acetonitrile were deoxygenated with a stream of argon gas. For the measurements on $[\mathbf{2}]^{2+}$, $\mathrm{CH_2Cl_2}$ was used as solvent, and the other conditions were same as for $[\mathbf{1}]^{8+}$. The reference electrode was Ag/AgCl against which the half-wave potential, $E_{1/2}$, of $\mathrm{Fc^+/Fc}$ was 0.43 V. All values of redox potentials refer to Ag/AgCl. For the measurement of emissive properties, the

---

(6) Takeuchi, K. J.; Thompson, M. S.; Pipes, D. W.; Meyer, T. J. *Inorg. Chem.* **1984**, *23*, 1845−1851.

(7) Fleischer, E. B.; Shachter, A. M. *Inorg. Chem.* **1991**, *30*, 3763−3769.

solutions were deoxygenated by purging with an argon gas stream for 15 min, and they were sealed before the measurements. The temperature of the solutions was controlled within ±1 °C by using a liquid N_2 cryostat (Oxford instruments, MODEL NO.010200). The temperature dependence of the emission spectra was measured with a multichannel photodetector (Hamamatsu, PMA-11) and a Ti:sapphire laser (Coherent, Mira Model 900-F) at 400 nm excitation. Emission decay profiles were measured with a microchannel-plate photomultiplier (Hamamatsu, R3809U-50), equipped with a monochromator (Jobin Ybon, H-20), and analyzed by a single-photon counting module (Edinburgh Instruments, SPC-300). Time-resolved and transient absorption spectra were measured by a polychlomator (Oriel, MULTISPEC 257)-multichannel photodetector (Oriel, INSTASPEC V) set and a Nd:YAG laser (Continuum, Surelite II) at 355 nm excitation.

X-ray Diffraction Studies. Suitable single crystals of [**1**]$(PF_6)_8$ were obtained from acetone−chloroform solutions as described in the preparation section. The measurement was performed at −120 °C because the crystal solvents were easy to be released at room temperature. The selected crystals were mounted onto a thin glass fiber. Measurement was made on a Mercury CCD area detector coupled with a Rigaku AFC-8S diffractometer with graphite monochromated Mo Kα radiation. Final cell parameters were obtained from a least-squares analysis of reflections with $I > 10\sigma(I)$. Space group $P\bar{1}$ resulted in the successful solution and refinement of the structures. Data were collected at a temperature of −120 °C to a maximum 2θ value of 55°. Data were collected in 0.5° oscillations (in ω) with 60.0 s exposures (in two 30.0 s repeats to allow dezingering). Sweeps of data were done using ω oscillations from −70 to 110° at $\chi = 45.0°$ and $\phi = 0.0°$ and from −20 to 60° at $\chi = 45.0°$ and $\phi = 90.0°$. The crystal-to-detector distance was 50.0 mm, and the detector swing angle was 20.0°. Data were collected and processed using Crystal Clear.[8] An empirical absorption correction resulted in acceptable transmission factors. The data were corrected for Lorentz and polarization factors.

All the calculations were carried out on a Silicon Graphics O2 computer system using teXsan.[9] The structures were solved by direct methods and expanded using Fourier and difference Fourier techniques. The crystal contains chloroform and acetone molecules as crystal solvents. Details of crystal parameters and structure refinement are given in Table 1. Selected bond lengths and angles are shown in Table 2.

Results

X-ray Crystal Structure of [1]$(PF_6)_8$. Figure 1 shows the structure of complex cation $[\mathbf{1}]^{8+}$.

This is the first X-ray structure of the molecular tetrapyridyl porphyrin complex with four surrounding nonporphyrin metal centers.[10,11] The porphyrin ring is essentially planer (maximum deviation from average plane is 0.11 Å) with four $\{Ru(bpy)(trpy)\}^{2+}$ units combining to four pyridyl groups (Ru−N distances of 2.109 and 2.121 Å). The bond distances within the H_2Py_4P and $\{Ru(bpy)(trpy)\}^{2+}$ units are in the range of distances found in related complexes.[12] The structure of the complex can be regarded as a large plane with a size of ca. 2 × 2 nm. For the arrangement of the four $\{Ru(bpy)(trpy)\}^{2+}$ units, complex cation $[\mathbf{1}]^{8+}$ adopted an approximate D_{2h} structure. The distances between the ruthenium atoms and the average plane of porphyrin are 0.62 and 0.93 Å in the crystal. The deviation from the ideal D_{2h} structure is caused by the rotation of the $\{Ru(bpy)(trpy)\}^{2+}$ units around the Ru−N(H_2Py_4P) bonds. Because the distances between the $\{Ru(bpy)(trpy)\}^{2+}$ units are far enough as shown in Figure 1, the rotation of the $\{Ru(bpy)(trpy)\}^{2+}$ units should occur to adjust the intermolecular van der Waals interaction.

Table 1. Crystallographic Data for [**1**]$(PF_6)_8 \cdot 4.83CHCl_3 \cdot 1.75CH_3COCH_3$

formula	$C_{160.17}H_{132.67}Cl_{29}F_{48}N_{28}O_{3.50}P_8Ru_4$
mw	5097.79
temp (°C)	−120
cryst syst	triclinic
space group	$P\bar{1}$
a (Å)	13.3333(4)
b (Å)	18.5426(5)
c (Å)	21.7336(2)
α (deg)	76.032(7)
β (deg)	72.085(6)
γ (deg)	85.699(8)
V (Å^3)	4961.6(3)
Z	1
μ (mm^{-1})	0.857
d_{calcd} (g cm^{-3})	1.706
no. of unique reflns (R_{int})	19 020 (0.023)
no. of obsd reflns	14 728, $I > 2\sigma(I)$
no. of params	1263
R1, wR2[a]	0.0832, 0.2327

[a] $R1 = \sum||F_o| - |F_c||/\sum|F_o|$; $wR2 = \{\sum[w(F_o^2 - F_c^2)^2]/\sum[w(F_o^2)^2]\}^{1/2}$ with $w = \{\sigma^2(F_o^2) + [x(\max(F_o^2, 0) + 2F_c^2)/3]^2\}^{-1}$.

Table 2. Selected Bond Distances (Å) and Angles (deg) for [**1**]$(PF_6)_8 \cdot 4.83CHCl_3 \cdot 1.75CH_3COCH_3$

Ru1−N3	2.121(4)	Ru2−N4	2.109(5)
Ru1−N5	2.079(6)	Ru2−N10	2.065(6)
Ru1−N6	1.966(5)	Ru2−N11	1.957(5)
Ru1−N7	2.070(6)	Ru2−N12	2.066(5)
Ru1−N8	2.062(5)	Ru2−N13	2.044(5)
Ru1−N9	2.068(5)	Ru2−N14	2.105(5)
N3−Ru1−N5	87.6(2)	N4−Ru2−N10	88.5(2)
N3−Ru1−N6	84.7(2)	N4−Ru2−N11	89.3(2)
N3−Ru1−N7	93.8(2)	N4−Ru2−N12	93.6(2)
N3−Ru1−N8	173.9(2)	N4−Ru2−N13	173.4(2)
N3−Ru1−N9	97.0(2)	N4−Ru2−N14	96.7(2)

^{1}H NMR. The ^{1}H NMR spectra of $[\mathbf{1}]^{8+}$ and $[\mathbf{2}]^{2+}$ are complicated because of the presence of various type of pyridyl rings from pyridyl porphyrins, trpy, and bpy. Assignments have been made by the comparison with the spectra of the free-base porphyrin, H_2PyT_3P, and the ruthenium unit analogue, $[Ru(bpy)(trpy)(py)]^{2+}$ (py = pyridine), and the two-dimensional ^{1}H NMR spectroscopies.

---

(8) *Crystal Clear*; Rigaku Corp.: Tokyo, 1999.

(9) *teXsan*, version 1.11; Molecular Structure Corporation: The Woodlands, TX, 2000.

(10) Konarev, D. V.; Litvinov, A. L.; Neretin, I. S.; Drichko, N. V.; Slovokhotov, Y. L.; Lyubovskaya, R. N.; Howard, J. A. K.; Yufit, D. S. *Cryst. Growth Des.* **2004**, *4,* 643−646.

(11) (a) Kumar, R. K.; Goldberg, I. *Angew. Chem., Int. Ed.* **1998**, *37,* 3027−3030. (b) Sondaz, E.; Gourdon, A.; Launay, J.-P.; Bonvoisin, J. *Inorg. Chim. Acta* **2001**, *316,* 79−88. (c) Mosher, P. J.; Yap, G. P. A.; Crutchley, R. J. *Inorg. Chem.* **2001**, *40,* 1189−1195. (d) Mosher, P. J.; Yap, G. P. A.; Crutchley, R. J. *Inorg. Chem.* **2001**, *40,* 550−553. (e) Konno, H.; Kobayashi, A.; Sakamoto, K.; Fagalde, F.; Katz, N. E.; Saitoh, H.; Ishitani, O. *Inorg. Chim. Acta* **2000**, *299,* 155−163. (f) Rasmussen, S. C.; Ronco, S. E.; Mlsna, D. A.; Billadeau, M. A.; Pennington, W. T.; Kolis, J. W.; Petersen, J. D. *Inorg. Chem.* **1995**, *34,* 821−829. (g) Nagao, H.; Mizukawa, T.; Tanaka, K. *Inorg. Chem.* **1994**, *33,* 3415−3420.

(12) Hecker, C. R.; Fanwick, P. E.; McMillin, D. R. *Inorg. Chem.* **1991**, *30,* 659−666.

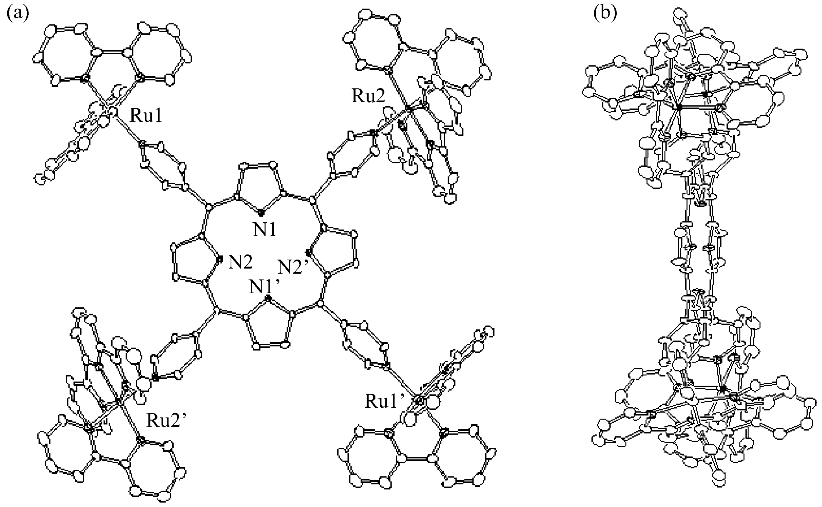

Figure 1. ORTEP drawing of complex cation [**1**]$^{8+}$: (a) top view and (b) side view.

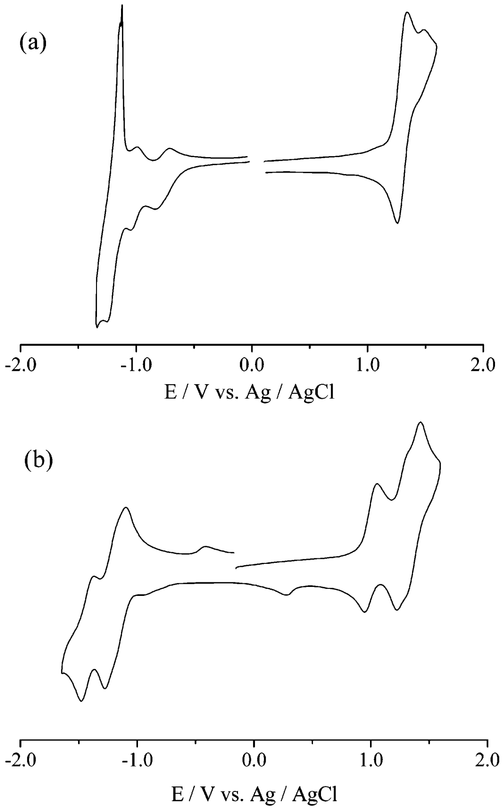

Figure 2. Cyclic voltammograms for (a) [**1**]$^{8+}$ in CH_3CN and (b) [**2**]$^{2+}$ in CH_2Cl_2.

The spectrum was not obtained for H_2Py_4P because of its poor solubility. In the ^1H NMR spectrum of [**1**]$^{8+}$, the signals of the four pyridyl groups of H_2Py_4P are observed as one set, as well as those of four {Ru(bpy)(trpy)}$^{2+}$ units, showing that the distorted structures observed in the crystals are not retained in solution and are not from the intramolecular interactions.

Cyclic Voltammograms. Cyclic voltammograms of [**1**]$^{8+}$ and [**2**]$^{2+}$ were measured in acetonitrile and dichloromethane, respectively (Figure 2). The redox potentials are listed in Table 3 along with those of the related compounds.

The redox behavior of [**2**]$^{2+}$ is interpreted as a sum of those of the components (Figure 2b). Those of the ruthenium unit may be referred to that of the pyridine analogue, [Ru(bpy)(trpy)(py)]$^{2+}$, which shows reversible one-electron oxidation and reduction waves at +1.36 V and at −1.19 V, assignable to the oxidation of Ru^{II} and the reduction of trpy, respectively. The free-base porphyrin, H_2PyT_3P, shows the redox waves at +1.25, +1.00, −1.21, and −1.52 V. All the redox waves of the components are observed at almost the same potentials in the cyclic voltammogram of [**2**]$^{2+}$.

For [**1**]$^{8+}$, five redox processes were observed, as shown in Table 3. Among them, the three waves at +1.48, −0.78, and −1.02 V showed a much lower current intensity than the rest (approximately 1:4). Thus, the former and latter redox processes should be attributed to the porphyrin and ruthenium units, respectively. The redox potentials attributed to ruthenium units were almost identical with those in [**2**]$^{2+}$ and [Ru(bpy)(trpy)(py)]$^{2+}$. Although the redox potential of the free H_2Py_4P was not measurable because of its poor solubility, the more positive values of H_2Py_4P in [**1**]$^{8+}$ than those of H_2PyT_3P in [**2**]$^{2+}$ should be attributed to the increase of pyridyl groups in H_2Py_4P.[2c] The redox potentials of H_2Py_4P in [{Os(OEP)(CO)}$_4$(μ_4-H_2Py_4P)] were observed at similar potentials (+1.37, −0.82 and −1.32 V) to those in [**1**]$^{8+}$, showing that the redox potentials of the H_2Py_4P ligand related to the central porphyrin unit is not significantly perturbed in this type of complexes. Accordingly, the redox behavior of [**1**]$^{8+}$ can also be interpreted as the sum of the components. Beccause of the positive shift of redox potentials of H_2Py_4P compared to H_2PyT_3P, the HOMO level of the H_2PyT_3P unit is higher than that of the {Ru(bpy)(trpy)}$^{2+}$ unit, while that of H_2Py_4P is lower than that of the {Ru(bpy)(trpy)}$^{2+}$ unit, and the LUMO of the H_2PyT_3P unit lies lower than that of H_2Py_4P.

Since the redox potentials observed for [**2**]$^{2+}$ and [**1**]$^{8+}$ are similar to those of the constituents, the electronic interactions between the porphyrin and ruthenium units in the complexes are not large enough to change the HOMO and LUMO levels in each component. Also, no sign of

Table 3. Oxidation and Reduction Potentials of the Complexes. (V vs Ag/AgCl)

	Ru component		porphyrin component				
	$Ru^{II/III}$ (ΔE_p)	$trpy^{0/-}$ (ΔE_p)	$Por^{0/+}$ (ΔE_p)	$Por^{+/2+}$ (ΔE_p)	$Por^{-/0}$ (ΔE_p)	$Por^{2-/-}$ (ΔE_p)	solvent
$[Ru(bpy)(trpy)(py)](PF_6)_2$	+1.36 (0.10)	−1.19 (0.08)					CH_2Cl_2
H_2PyT_3P			+1.00 (0.07)	+1.25 (0.06)	−1.21 (0.11)	−1.52 (0.10)	CH_2Cl_2
[**1**]$(PF_6)_8$	+1.30 (0.08)	-1.25^{a}	$+1.48^{b}$		−0.78 (0.13)	−1.02 (0.05)	CH_3CN
[**2**]$(PF_6)_2$	+1.38 (0.11)	−1.15 (0.26)	+0.99 (0.08)	+1.26 (0.09)	−1.15 (0.26)	−1.43 (0.11)	CH_2Cl_2

[a] E_{pc}. [b] E_{pa}.

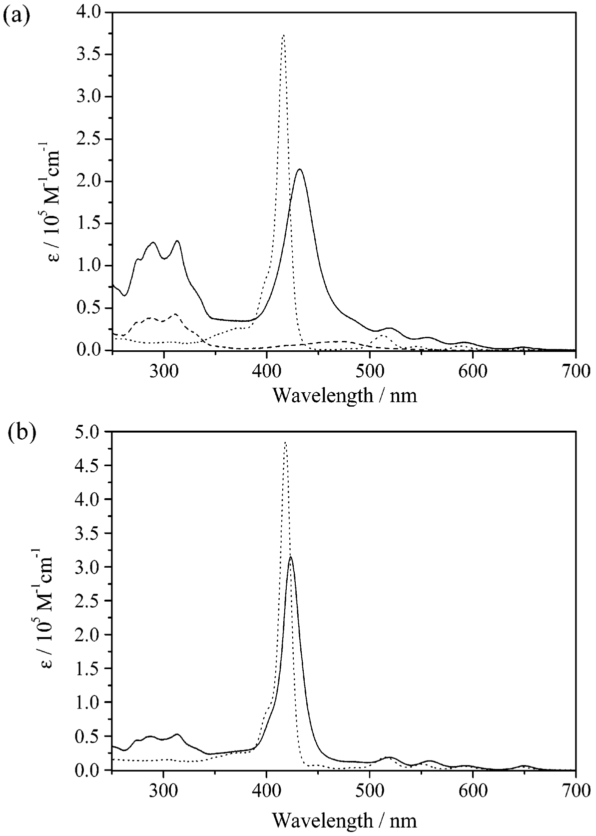

Figure 3. (a) Room-temperature UV−vis absorption spectra of $[\mathbf{1}]^{8+}$ (solid line), $[Ru(bpy)(trpy)(pyridine)]^{2+}$ (dashed line), and H_2Py_4P (dotted line) in CH_2Cl_2. (b) Room-temperature UV−vis absorption spectra of $[\mathbf{2}]^{2+}$ (solid line) and H_2PyT_3P (dotted line) in CH_2Cl_2.

Table 4. Absorption and Emission Maxima (nm) of the Complexes[a]

	absorption		emission	
	Ru component	porphyrin component	Ru component	porphyrin component
$[Ru(bpy)(trpy)(py)](PF_6)_2$	313, 476		603	
H_2Py_4P		416, 512, 545, 587, 643		645, 709
H_2PyT_3P		418, 515, 550, 591, 646		649, 714
[**1**]$(PF_6)_8$	313	432, 519, 556, 591, 648	624^{b}	649, 712, 834^{b}
[**2**]$(PF_6)_2$	313	423, 519, 568, 593, 650		655, 716

[a] Measured at room temperature in CH_2Cl_2. [b] Measured at 77 K in EtOH/MeOH.

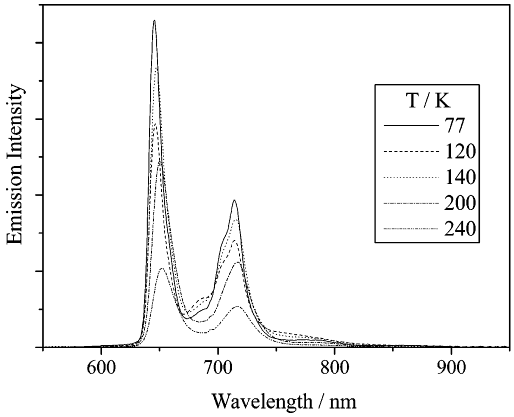

Figure 4. Emission spectra of $[\mathbf{2}]^{2+}$ at varying temperatures. The excitation wavelength is 400 nm.

splitting of the redox waves for the ruthenium units in $[\mathbf{1}]^{8+}$ shows that the redox interaction through the central porphyrin is not large enough to stabilize the mixed-valence complexes, as observed in the complexes bridged by pyrazine or 4,4′-bpy.[13] Thus, construction of the supramolecule framework with pyridyl porphyrin allows direct connection between the units, retaining the redox properties of each unit.

UV−Vis Absorption Spectra. UV−vis absorption spectra of $[\mathbf{1}]^{8+}$ and $[\mathbf{2}]^{2+}$ in CH_2Cl_2 (Figure 3) are dominated by a strong Soret band of the porphyrin moieties.

Free-base porphyrins, H_2Py_4P and H_2PyT_3P, give Soret bands at 416 (full width at half-maximum (fwhm) = 14 nm) and 418 nm (fwhm = 16 nm), respectively (Table 4). Upon complexation to the $\{Ru(bpy)(trpy)\}^{2+}$ unit, the bands shift to a longer wavelength with considerable broadening.[5(a),14] Thus, $[\mathbf{1}]^{8+}$ and $[\mathbf{2}]^{2+}$ have bands at 432 (fwhm = 37 nm) and 423 nm (fwhm = 21 nm), respectively. As the extent of the shift and the broadening is more extensive for $[\mathbf{1}]^{8+}$, electronic interaction between the porphyrin and the ruthenium units is evident. The $\pi-\pi^*$ transition of the $\{Ru(bpy)(trpy)\}^{2+}$ unit was observed coincidentally around 300 nm for both $[\mathbf{1}]^{8+}$ and $[\mathbf{2}]^{2+}$. The extinction coefficient of this band for $[\mathbf{1}]^{8+}$ was about four times larger than that for $\{Ru(bpy)(trpy)\}^{2+}$, reflecting the number of $\{Ru(bpy)(trpy)\}^{2+}$ units in the molecule.

Emissive Properties. Figure 4 shows the emission spectra of $[\mathbf{2}]^{2+}$ in ethanol/methanol (4:1 v/v).

The complex shows a weak emission typical for the porphyrin moiety (centered at 655 and 716 nm), and its intensity increases as the temperature decreases. At room

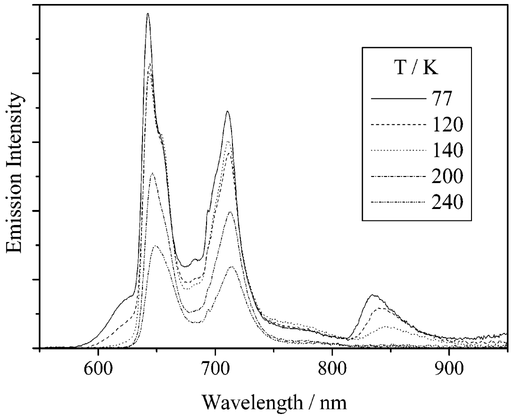

Figure 5. Emission spectra of $[\mathbf{1}]^{8+}$ at varying temperatures. The excitation wavelength is 400 nm.

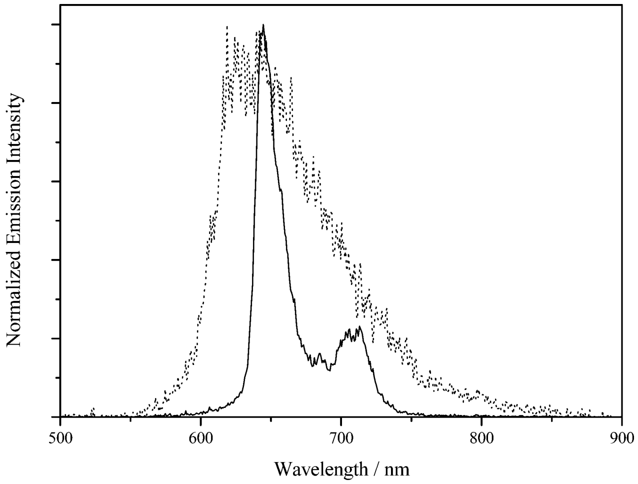

Figure 6. Time-resolved emission spectra of $[\mathbf{1}]^{8+}$ at 77 K: 0−15 ns (solid line) and 15−200 ns (dashed line). The excitation wavelength is 355 nm.

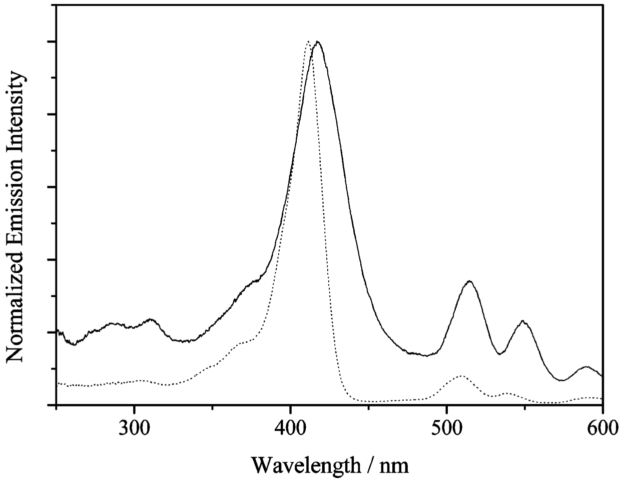

Figure 7. Excitation spectra of $[\mathbf{1}]^{8+}$ (solid line) and H_2Py_4P (dotted line) in CH_2Cl_2. The emission wavelength is 650 nm.

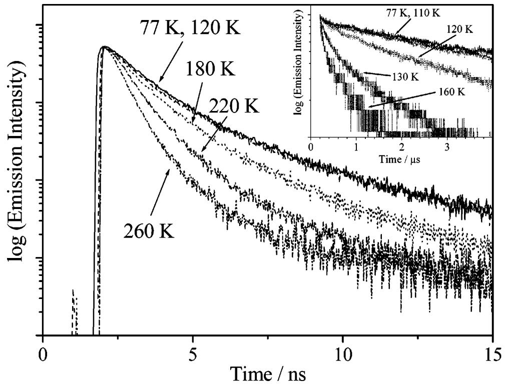

Figure 8. Emission decays of $[\mathbf{1}]^{8+}$ at various temperatures in the nanosecond range. The inset shows the decays in the microsecond range. The excitation wavelength is 400 nm. The fitting parameters are listed in Tables S1 and S2.

temperature, complex $[\mathbf{1}]^{8+}$ in ethanol/methanol (4:1 v/v) also shows weak singlet emissions, centered at 649 and 712 nm, of the porphyrin ring (Figure 5 and Table 4).

The emission becomes stronger as the temperature decreases, and in contrast to $[\mathbf{2}]^{2+}$, additional features appeared below ca. 140 K. At 77 K, in addition to the room-temperature features, broad emissions from the ruthenium moiety in the region of 600−800 nm and porphyrin phosphorescence at 834 nm are unambiguously observed.[5a,15] Figure 5 shows that the ruthenium and porphyrin triplet emissions appear concurrently. Time-resolved emission spectra (Figure 6) clearly show that the porphyrin fluorescence and ruthenium phosphorescence have significantly different lifetimes. While the porphyrin fluorescence disappears within 15 ns, the ruthenium emission stays in the spectrum in the range of 15−100 ns.

Figure 7 shows the excitation spectrum of $[\mathbf{1}]^{8+}$ at room temperature.

The features corresponding to the porphyrin absorption spectrum were observed with strong band at 418 nm (corresponding to the Soret band) and somewhat weaker bands at 515 and 549 nm (corresponding to the Q band). The Q band features are relatively strong, compared with the absorption spectrum of $[\mathbf{1}]^{8+}$. The excitation bands at 285 and 310 nm (corresponding to the $\pi-\pi^*$ transition in the $\{Ru(bpy)(trpy)\}^{2+}$ unit) are also observed, but they are considerably weak. The estimated quantum yield for the irradiation light at 310 nm ($\pi-\pi^*$ transition in the $\{Ru(bpy)(trpy)\}^{2+}$ unit) is 0.0009, while that at 550 nm (the Q band) is 0.004.[16]

Figure 8 shows the emission decay of $[\mathbf{1}]^{8+}$ at various temperatures, which we were not able to fit with a single exponential.

At room temperature, the major part of the fluorescence decays with the lifetime of 340 ps with the contribution of some minor component (617 ps, 18%).[17] The emission is considerably weaker, and the lifetime is much shorter than the fluorescence of the free porphyrin H_2Py_4P (8.28 ns) in CH_2Cl_2. The lifetime of the fluorescence of $[\mathbf{1}]^{8+}$ increases

---

(13) (a) Creutz, C. *Prog. Inorg. Chem.* **1983**, *30*, 1−73. (b) Powers, M. J.; Meyer, T. J. *J. Am. Chem. Soc.* **1973**, *95*, 1086−1094.

(14) Prodi, A.; Kleverlaan, C. J.; Indelli, M. T.; Scandola, F.; Alessio, E.; Iengo, E. *Inorg. Chem.* **2001**, *40*, 3498−3504.

(15) (a) Kalyanasundaram, K. *Chem. Phys. Lett.* **1984**, *104*, 357−362. (b) Quimby, D. J.; Longo, F. R. *J. Am. Chem. Soc.* **1975**, *97*, 5111−5117.

(16) Emission quantum yields of the complexes were estimated by using H_2Py_4P ($\phi_{em} = 0.072$) as a standard, see ref 21.

(17) To estimate the lifetime of the excited state, the decays were fit with a double exponential (Figures S1 and S2). Tables S1 and S2 list the fitting parameters.

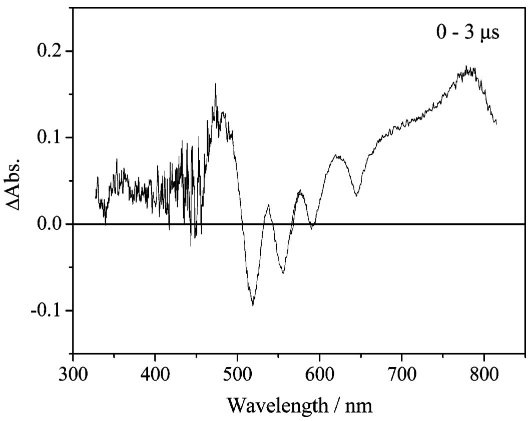

Figure 9. Transient absorption difference spectrum of [**1**]$^{8+}$ at room temperature in the time range of 0−3 μs. The excitation wavelength is 355 nm.

with the decrease in temperature, and the lifetime was 1.08 ns at 77 K. The phosphorescence from the ruthenium moiety observed at lower temperatures shows much longer lifetime (3.67 μs at 77 K).

Transient Absorption Spectra. The transient absorption spectrum (0−3 μs) of [**1**]$^{8+}$ at room temperature (Figure 9) shows the weak features of the porphyrin triplet state ($^3H_2Py_4P$),[18] although [**1**]$^{8+}$ did not show the porphyrin phosphorescence at room temperature.

The decay lifetime as observed by the transient absorption spectra was 160 μs. The absorption of the ruthenium triplet excited state (^{3}MLCT)[4,19] was hardly apparent in the transient absorption spectrum of [**1**]$^{8+}$ at room temperature. Thus, although the triplet emissions were observed from both the porphyrin and ruthenium moieties at low temperatures, the triplet excited state at room temperature may be located on the porphyrin site.

Discussion

The detailed analysis of the energetics of the present system provides information on energy transfer among adjacent components having energetically similar excited states. Since all the three possible emissions occur in a single emission spectrum, further detailed discussion of the excited-state profiles becomes possible. At lower temperatures (<140 K), complex [**1**]$^{8+}$ showed porphyrin singlet and triplet emissions, as well as ruthenium emission.The small energy difference allows the simultaneous population of three possible states. This is the first unambiguous observation of porphyrin and ruthenium phosphorescence simultaneously in any porphyrin−ruthenium(polypyridyl) hybrid system.

Araki, Toma, and co-workers have previously studied the photophysical behavior of two similar 1:4 porphyrin−ruthenium(polypyridyl) hybrid systems where porphyrins were metalated by Zn^{2+}.[5] One of the complexes, $[Ru(bpy)_2Cl]_4\{Zn(Py_4P)\}^{4+}$, shows porphyrin phosphorescence centered at 770 nm at 77 K in ethanol glass, in addition to its fluorescence.[5] Very weak ruthenium emission was suggested to be observed in this case.[20] The excitation spectrum of the porphyrin phosphorescence is featured by the strong ruthenium absorption. It was suggested that the ^{3}MLCT of the ruthenium moiety was quenched through an intramolecular energy-transfer mechanism by the porphyrin moiety to give $^3ZnPy_4P$. The other system was constructed with a porphyrin whose meso sites are connected by 5-methyl-2,2′-bipyridine units at the 5′-carbon (H_2bpy_4P), providing chelating ability to the porphyrin meso substituent.[5] The 1:4 hybrid, $[Ru(bpy)_2]_4\{Zn(bpy_4P)\}^{8+}$, showed ruthenium emission, in addition to the minor contribution of the porphyrin fluorescence at room temperature. Thus, the ruthenium ^{3}MLCT state appears to be the lowest excited state. Upon the addition of imidazole as an axial ligand of the Zn porphyrin unit, only the porphyrin fluorescence was observed. The coordination of imidazole to Zn^{2+} significantly lowers the π^* level of the porphyrin unit which is now the lowest-excited state. These studies indicate that the excited-state energy levels of porphyrin and ruthenium units are very close and can be easily reversed by the introduction of substituents and the axial coordination to the metal ions in the porphyrin ring.

The energy level diagrams of complex [**1**]$^{8+}$ obtained from the photophysical results are summarized in Figure 10. The estimated energies of excited states are listed in Table 5.

As shown in Figure 5, in the room-temperature emission spectrum of [**1**]$^{8+}$, no emission from the ruthenium unit and only a weak fluorescence from the porphyrin singlet state ($(^1H_2Py_4P)_1$) was observed. The quantum yield of [**1**]$^{8+}$ (0.004) is lower than that of free H_2Py_4P (0.072).[21] Thus, the emissions of the ruthenium and porphyrin units are effectively quenched in [**1**]$^{8+}$. It has been reported that the efficient electron-transfer quenching takes place in the porphyrin−Ru polypyridyl systems when their redox potentials are sufficiently separated. In this system, a charge-separated state ($Ru(III){-}H_2Py_4P^-$) is evaluated to exist proximately to both the ^{3}MLCT of the ruthenium units and the $(^1H_2Py_4P)_1$. Therefore, the electron-transfer quenching by $Ru(III){-}H_2Py_4P^-$ should plausibly be the dominant pathway to quench the emissions from ^{3}MLCT and $(^1H_2Py_4P)_1$, even though the energy transfer to $(^1H_2Py_4P)_1$ and $^3H_2Py_4P$ takes place (vide infra).[22]

The room-temperature excitation spectrum of [**1**]$^{8+}$ (emission at 650 nm) shows weak peaks at 285 and 310 nm in addition to the strong visible features of the porphyrin moieties. Because the bands at around 300 nm are mainly

---

[18] (a) Pekkarinen, L.; Linschitz, H. *J. Am. Chem. Soc.* **1960**, *82*, 2407−2411. (b) Asano-Someda, M.; Kaizu, Y. *Inorg. Chem.* **1999**, *38*, 2303−2311. (c) Flamigni, L.; Barigelletti, F.; Armaroli, N.; Ventura, B.; Collin, J.-P.; Sauvage, J.-P.; Williams, J. A. G. *Inorg. Chem.* **1999**, *38*, 661−667.

[19] Wallin, S.; Davidsson, J.; Modin, J.; Hammarström, L. *J. Phys. Chem. A* **2005**, *109*, 4697−4704.

[20] Although the authors reported that "a broad weak band was observed at 680 nm" for $[Ru(bpy)_2Cl]_4\{Zn(Py_4P)\}^{4+}$ in ref 5a, the band they mentioned was so weak that it was hard to distinguish from the fluctuation of the baseline.

[21] Kalyanasundaram, K. *Inorg. Chem.* **1984**, *23*, 2453−2459.

[22] The energy transfer from ^{3}MLCT to $^3H_2Py_4P$ is also attributed to the quenching of emission from ^{3}MLCT (see Benniston, A. C.; Chapman, G. M.; Harriman, A.; Mehrabi, M. *J. Phys. Chem. A* **2004**, *108*, 9026−9036). However, the emission from ^{3}MLCT at low temperature may not be observed if this process is efficient in the present system. A more detailed examination of the quenching pathway is now underway with various redox potentials for the components.

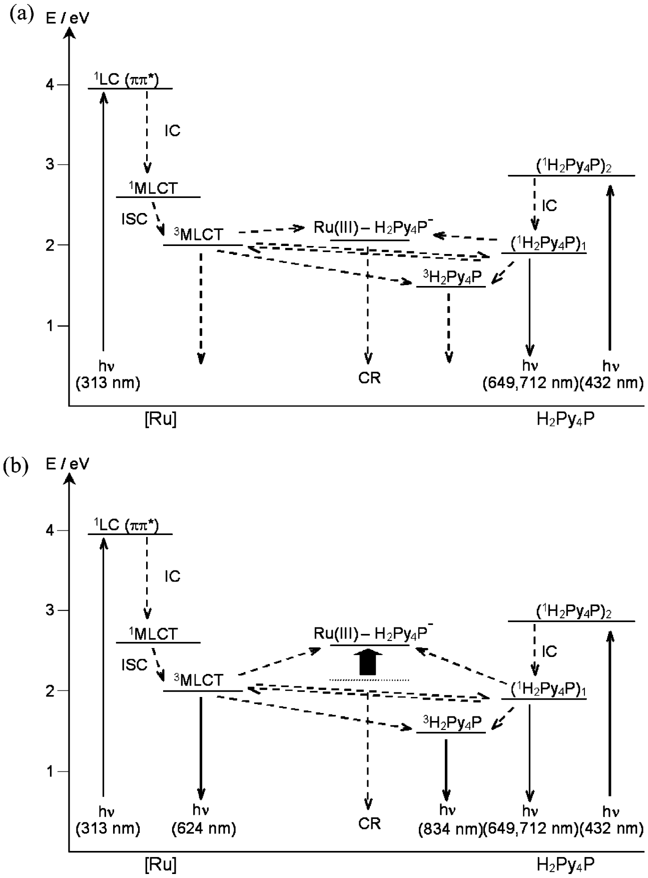

Figure 10. Schematic energy level diagrams and photoinduced processes for [**1**]$^{8+}$ (a) at room temperature and (b) at 77 K. The solid lines represent radiative transitions, and the dashed lines represent nonradiative transitions (IC, internal conversion; ISC, intersystem crossing; CR, charge recombination).

Table 5. Energies of Excited States for [**1**](PF$_6$)$_8$ and [**2**](PF$_6$)$_2$

[**1**](PF$_6$)$_8$		[**2**](PF$_6$)$_2$	
state	*E* (eV) (wavelength (nm))	state	*E* (eV) (wavelength (nm))
^{1}LC	3.96 (313)^a	^{1}LC	3.96 (313)^a
^{3}MLCT	1.99 (624)^c	(^{1}H$_2$PyT$_3$P)$_2$	2.93 (423)^a
(^{1}H$_2$Py$_4$P)$_2$	2.87 (432)^a	(^{1}H$_2$PyT$_3$P)$_1$	1.89 (655)^b
(^{1}H$_2$Py$_4$P)$_1$	1.91 (649)^b	trpy$^-$−H$_2$PyT$_3$P$^+$	2.14^d
^{3}H$_2$Py$_4$P	1.49 (834)^c		
Ru^{III}−H$_2$Py$_4$P$^-$	2.08^d		

[a] Estimated from absorption maxima. [b] Estimated from emission maxima at room temperature. [c] Estimated from emission maxima at 77 K. [d] Estimated from redox potentials.

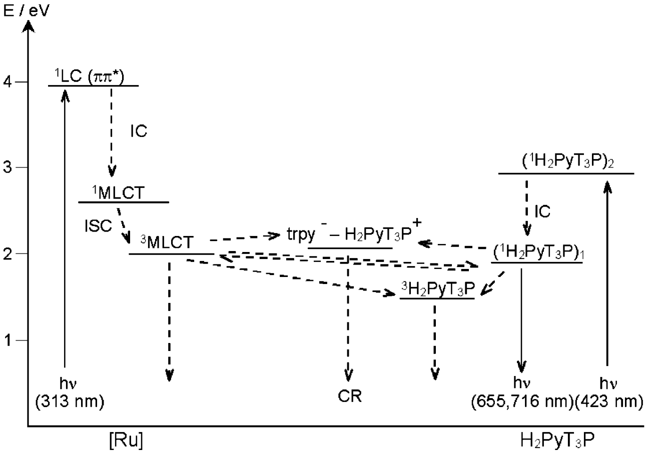

Figure 11. Schematic energy level diagrams and photoinduced processes for [**2**]$^{2+}$. The solid lines represent radiative transitions, and the dashed lines represent nonradiative transitions (IC, internal conversion; ISC, intersystem crossing; CR, charge recombination).

based on the ligand-centered (^{1}LC) absorption of polypyridyl ligands in the ruthenium units, the existence of the bands in the excitation spectrum certifies the energy transfer from ruthenium units to emissive (^{1}H$_2$Py$_4$P)$_1$. Because of the efficient internal conversion and intersystem crossing processes from ^{1}LC to ^{3}MLCT in the ruthenium polypyridyl complexes,[23] the energy transfer observed here should be attributed to that from ^{3}MLCT to (^{1}H$_2$Py$_4$P)$_1$.[24] The small intensity of the bands in the excited spectrum suggests that the energy transfer from the ^{3}MLCT state to (^{1}H$_2$Py$_4$P)$_1$ has a minor contribution to the quenching process of the ^{3}MLCT state.

The room-temperature transient absorption spectrum of [**1**]$^{8+}$ shows the existence of the porphyrin triplet state (Figure 9), indicating that ^{3}H$_2$Py$_4$P was generated by the energy transfer from (^{1}H$_2$Py$_4$P)$_1$ by the heavy atom effect or by the energy transfer from ^{3}MLCT. The lack of phosphorescence from ^{3}H$_2$Py$_4$P is the result of the low emission efficiency at higher temperatures, as observed in other porphyrins.[25]

The emission spectra of [**1**]$^{8+}$ at low temperatures show not only porphyrin fluorescence but also porphyrin phosphorescence and {Ru} phosphorescence. At the low temperatures, below the freezing point, the charge-separated states are destabilized by the lack of solvent repolarization by at least 0.25 eV.[26] Such an energy increase of the charge-separated state suppresses the quenching by the electron-transfer pathway, resulting in emission from ^{3}MLCT state at low temperatures. The phosphorescence of H$_2$Py$_4$P is observed simultaneously, probably, because the rate of nonradiative decay of ^{3}H$_2$Py$_4$P decelerates as observed for other porphyrin systems.[18] The phosphorescence from ^{3}MLCT was observed upon excitation at 400 nm (Soret band). Therefore, energy transfer from (^{1}H$_2$Py$_4$P)$_1$ to ^{3}MLCT is also feasible.

The energy level diagram of complex [**2**]$^{2+}$ is shown in Figure 11. In [**2**]$^{2+}$, the emission spectra showed only fluorescence from (^{1}H$_2$PyT$_3$P)$_1$ at room and lower temperatures (Figure 4). The lack of phosphorescence from {Ru} unit even at low temperatures is explained by the stabilization of the (^{1}H$_2$PyT$_3$P)$_1$ state. The phosphorescence of ^{3}H$_2$PyT$_3$P was not observed in [**2**]$^{2+}$. It may be assumed that the heavy atom effect that is not sufficient to cause intersystem crossing in ^{3}H$_2$PyT$_3$P because [**2**]$^{2+}$ has only one ruthenium unit.

---

(23) Juris, A.; Balzani, V.; Barigelletti, F.; Campagna, S.; Belser, P.; Von Zelewsky, A. *Coord. Chem. Rev.* **1988**, *84*, 85−277.

(24) Direct energy transfer or electron transfer from ^{1}LC, ^{1}MLCT, or both to (^{1}H$_2$Py$_4$P)$_1$ is unlikely since ^{3}MLCT emission was observed at room temperature for the related Ru-pyridylporphyrin hybrid system (see ref 5b). There is no reason to assume exceptional direct quenches of ^{1}LC or ^{1}MLCT in the present cases (see ref 3 and Shin, E. J.; Kim, D. *J. Photochem. Photobiol. A* **2002**, *152*, 25−31).

(25) Eng, M. P.; Ljungdahl, T.; Andréasson, J.; Mårtensson, J.; Albinsson, B. *J. Phys. Chem. A* **2005**, *109*, 1776−1784.

(26) Harriman, A.; Odobel, F.; Sauvage, J.-P. *J. Am. Chem. Soc.* **1995**, *117*, 9461−9472.

To summarize the excited-state dynamics of [**1**]$^{8+}$, the triplet excited state of the ruthenium moieties and $(^1H_2PyT_3P)_1$ is effectively quenched in [**1**]$^{8+}$. By analysis of the excitation spectra and transient absorption spectra, as well as by comparison to related systems, we determined that the energy of ^{3}MLCT migrated to $(^1H_2PyT_3P)_1$ and $^3H_2PyT_3P$ and should largely be quenched by the porphyrin unit via an electron-transfer mechanism. At lower temperatures, the electron-transfer quenching is not effective, and emission from the ruthenium MLCT triplet state occurs. The results obtained here demonstrate that the properties of supramolecular systems composed of units with energetically similar excited states can be altered by the small differences of properties of the units and experimental conditions, such as temperatures. In other words, such flexible systems can be used to reflect the circumstances.

Acknowledgment. Financial support from a Grant-in-Aid (15036201) on the priority area of “Reaction Control of Dynamic Complexes” from the Ministry of Education, Culture, Sports, Science and Technology, Japan, is gratefully acknowledged.

Supporting Information Available: Crystallographic data for [**1**]$(PF_6)_8$ in CIF format, two figures of emission decays with fitting curves, and two tables of fitting parameters. This material is available free of charge via the Internet at http://pubs.acs.org.

IC0602852